AEA FUS 259

AEA Technology
Fusion
(UKAEA/Euratom Fusion Association)

MHD Control and ECCD in Compass-D

T N Todd and the COMPASS Team

January 1994

AEA Technology
Fusion

Culham, Abingdon
Oxfordshire OX14 3DB
United Kingdom
Telephone 0235 463534
Facsimile 0235 463414

Paper on MHD Control and ECCD in Compass-D by TomTodd and the Compass Team which was presented at the EPS Conference in Lisbon on the 26-30 July 1993 and is now ready for publication.

MHD Control and ECCD in Compass-D

T N Todd and the COMPASS Team

AEA Technology Fusion, Culham Laboratory (Euratom/UKAEAFusion Association) Abingdon, Oxon OX14 3DB UK

Abstract. Electron cyclotron current drive experiments have been carried out in Compass-D using a power of ~500kW at a frequency of 60GHz. The fundamental resonance was used and the waves were launched from the high field side of the torus through four mirror-antennae. Significant asymmetry in the loop voltage behaviour is observed when comparing co and counter current drive cases, suggesting a driven current ~15kA (in a plasma current of 130kA). The BANDIT-3D Fokker Planck code has been used to model these discharges, revealing a similar value for the predicted driven current at zero loop voltage but strong synergistic effects with the toroidal electric field at the ~0.4Volts/turn typical of the experiments. This synergy appears to be sufficient to explain the inferred net "co" current drive in most of the "counter" current drive shots. In H-mode discharges featuring a strongly asymmetric single null separatrix configuration, discrete ELM's sometimes produce sufficient relaxation of the current profile to cause loss of vertical control, leading to Vertical Displacement Events. Application of resonant magnetic perturbations (RMPs) of predominantly n=1 (with various low m values) is seen reliably to increase the frequency of the ELM's, although the exact mechanism underlying this effect has still to be elucidated. A real-time electronic neural network has been used for the first time for feedback control of the equilibrium in a tokamak. The neural network was used for feedback control of the plasma elongation throughout the discharge, while simultaneously monitoring the plasma vertical and horizontal position.

Keywords. ECRH, ECCD, current drive, fundamental, electric field synergy, ELM, VDE, helical fields, resonant magnetic perturbation, neural network.

1. Introduction

Compass-D was commissioned in May 1992, moving rapidly from early trials with circular plasmas to high elongation (κ=1.9) D-shaped plasmas with significant triangularity (δ~0.5). Double-null separatrix configurations with the same elongation and negligible triangularity were also achieved. Activity in recent months has established routine operation with substantially asymmetric single null x-point (SNX) discharges very similar in magnetic topology to those proposed for ITER, as indicated in figure 1. The diverted magnetic field lines intercept a toroidal array of graphite tiles in the bottom of the vacuum vessel. The equilibrium parameters of these discharges are typified by R = 0.56m, a = 0.17m, κ = 1.6, δ = 0.3, $0.9<B\phi<2.0$T, $100\text{kA}<I_p<260\text{kA}$ with $q_\varphi 95 \approx 3 \rightarrow 10$. Key design features of the machine include 2MW of 60GHz ECRH, split evenly between high and low field side launch antennae (currently with 1.4MW installed capacity), and a highly adaptable set of resonant magnetic perturbation (RMP) windings with programmable current waveforms.

The machine is boronised using occasional glow discharge cleaning (GDC) in deuterated trimethyl boron ($(CD_3)_3B$), with GDC in helium every few shots to control recycling of the deuterium working gas. Very clear Ohmic H-modes, including various types of Edge Localised Mode (ELM) and ELM-free behaviour were discovered when high density SNX experiments were undertaken (see figure 2). ECRH H-modes have been achieved more recently, so far without ELM-free periods.

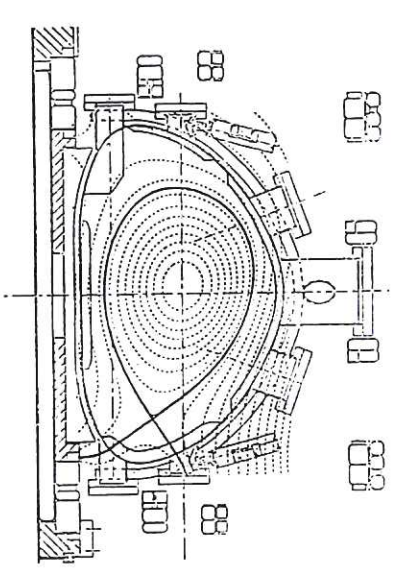

Figure 1. A typical SNX divertor configuration in Compass-D

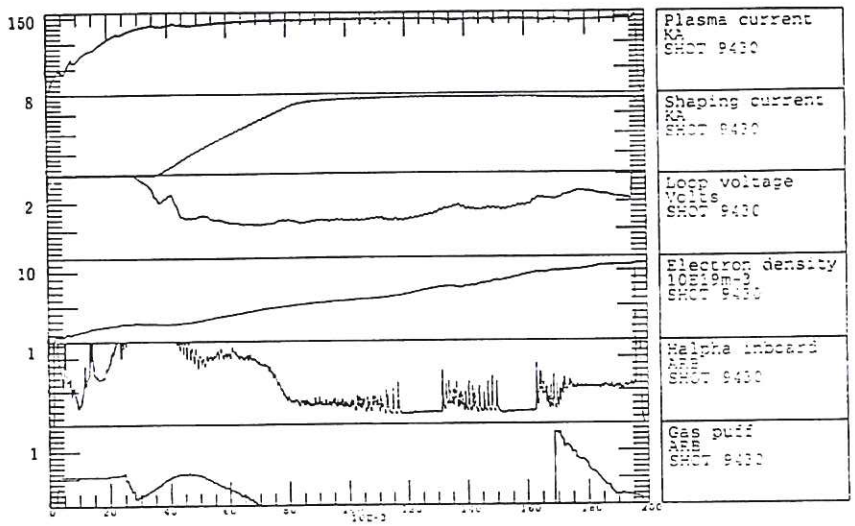

Figure 2. Waveforms of Ohmic H-mode separatrix plasma in Compass-D. Note the slow transition and development of ELM-free periods.

This paper will describe the use of the ECRH system for fundamental current drive experiments and also provisional results of the effect of RMP fields on ELM frequency in Ohmic H-mode plasmas. Some comments will also be made on n=0 MHD control in asymmetric plasmas, including the first use of an analogue electronic neural network for feedback control of the plasma elongation in a tokamak.

2. EC Current Drive

Four of the currently installed 60GHz ECRH lines utilise high field side launch mirror-antennae, each adjustable to any toroidal launch angle by rotation about the vertical axis of the input waveguide (see Fig 1). This allows experiments to be undertaken with a wide range of co and/or counter RF current drive. For Compass-D, the best compromise of current drive localisation and efficiency is achieved by the choice of fundamental resonance heating in the extraordinary mode (which comprises ~60% of the launched power for the present antenna design). Such experiments have been carried out using ≈500kW of ECRH with a toroidal field of 2.0T, in 130kA SNX discharges of fixed plasma current direction. The antenna patterns were centred on ±45° with respect to the major radius to optimise the current drive efficiency. The Doppler-shifted absorption zone for the ECRH is to the high field side of the cold resonance (B=2.14T), ie significantly to the inboard side of the torus, as shown in figure 3a.

Figure 3. ECRH ray tracing and Fokker Planck absorption analysis using BANDIT-3D.

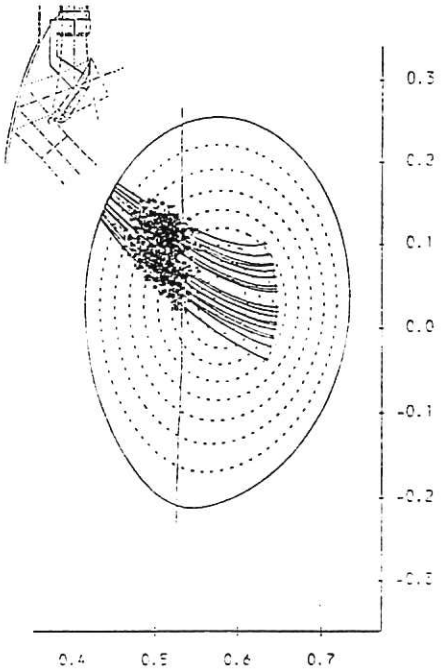

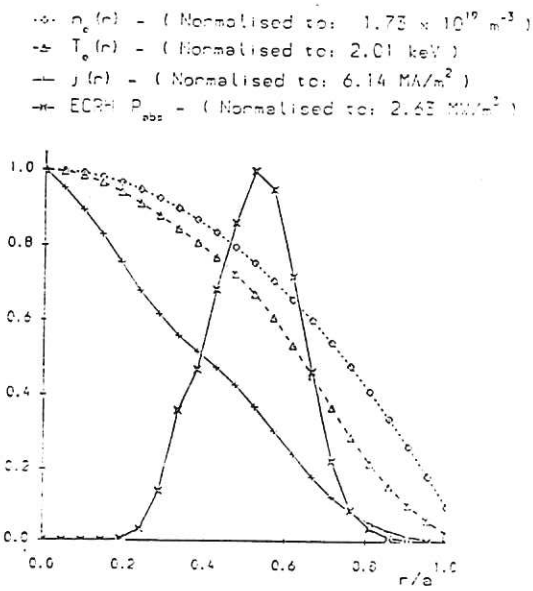

a) Ray tracing, showing regions of strong absorption, mostly before the waves reach the cold resonance (shown as a vertical line)

b) Predicted profiles of absorbed ECRH power and total current density, using the density and temperature profiles shown, 0.38V/turn in the co direction and $Z_{eff} = 1.5$

Figure 4 shows representative loop voltage traces for co and counter shots overlaid, clearly revealing a difference of ≈80mV/turn, compared to a mean value during the RF heating of ≈400mV/turn. Simply taking the RF-driven current as the total plasma current multiplied by half the fractional change in loop voltage would therefore imply a driven current ≈13kA, or 0.026A/W.

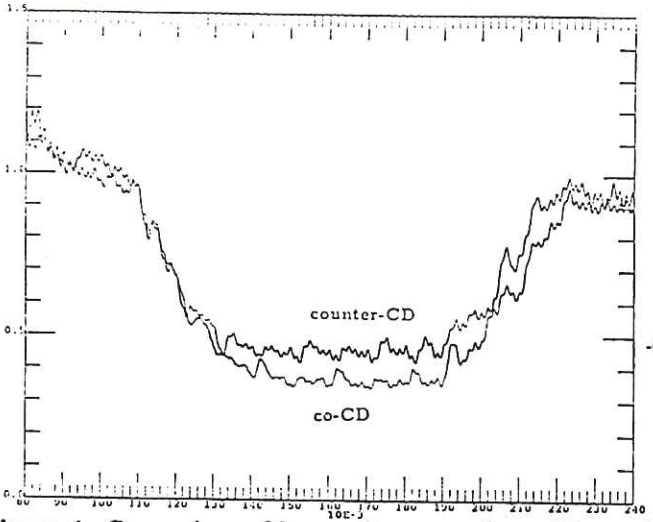

Figure 4. Comparison of loop voltage waveforms for co and counter current drive cases (500kW of ECRH launched at 45°, 130kA plasma current, $n_e \approx 1.2 \times 10^{19}$ m $^{-3}$)

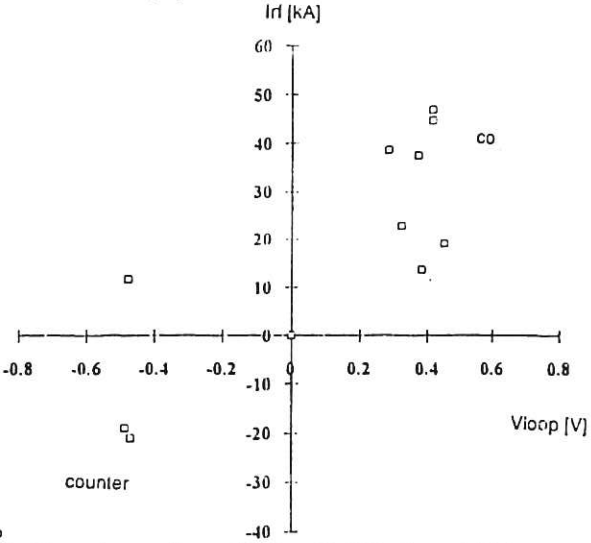

Figure 5. Experimental results for 60GHz $1\omega_{ce}$ ECCD in Compass-D, using changes in average resistivity $1\omega_{ce}$ inferred from diamagnetic and interferometric data. Positive current is defined as being in the direction the RF alone would generate; positive loop voltage means such that the ohmic heating current and the RF-alone current would be in the same direction.

However, a more detailed analysis reveals a more complex picture. In this latter approach, the driven current in each direction is independently estimated using the ansatz

$$I_{CD} = I_{TOT} - V_{Loop}/R_{Loop}$$

where R_{Loop} is estimated from

$$R_{Loop} = R_{Loop(OH)}\left[\frac{W_{dia}(OH)}{n_e(OH)}\ \frac{n_e}{W_{dia}}\right]^{\frac{3}{2}}$$

and it is assumed that average conductivity temperature is proportional to the diamagnetically determined stored energy divided by the line average electron density. This approach would be accurate if many un-measured parameters remained constant in the change from Ohmic heating to ECRH (eg. l_i, profile shapes, T_i/T_e, Z_{eff}, $\beta_\perp/\beta_\parallel$), most of which are in fact seen (or expected) to change somewhat. Nevertheless the results are informative, as indicated in figure 5, where it can be seen that some counter oriented shots seem to exhibit net co current drive.

This is at first sight unexpected but turns out to be representative of one class of results from 3D Fokker Planck modelling [1] summarised in figure 6.

Figure 6. Velocity-space plots of the plasma electron distribution function, with axis units normalised to $v_{thermal} = (2T_e/m_e)^{1/2}$, 300kW of RF power and the geometry , density and temperature profiles shown in figure 3. The dashed lines represent the boundaries between trapped and passing particles. a) Ohmic heating alone, b) ECR current drive alone (as though for a stellarator), c) ECR co current drive with OH, d) ECR counter current drive with OH.

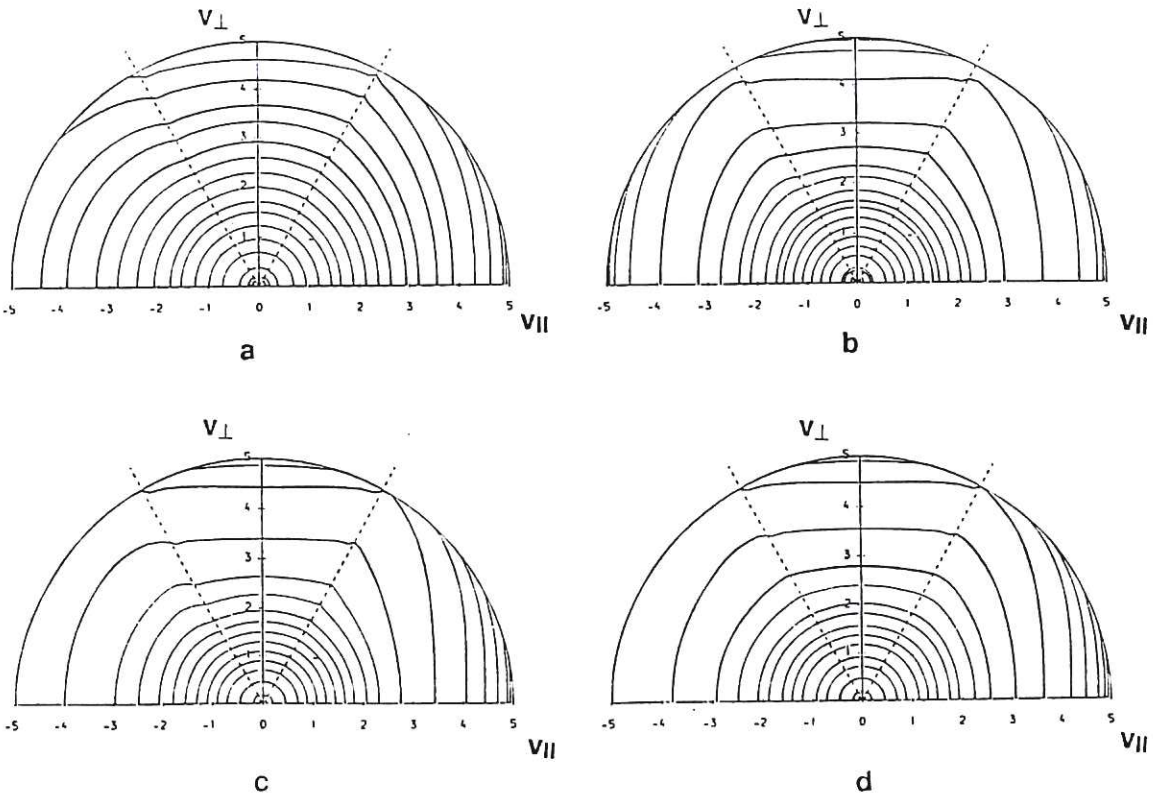

The code used is BANDIT-3D, which includes a self-consistent ray tracing and quasi-linear Fokker Planck operator for the effects of the ECRH, collisions, radial transport and particle trapping, and the ability to treat up-down asymmetric equilibria. The radial transport used in the runs featured a profile of diffusivity (D(r)) such that $n_e(r)D(r)$ - 10^{19}/metre-sec, with an inward pinch term adjusted to conserve the specified density profile. In order to facilitate comparisons, the temperature profile was kept the same for the various cases considered by arranging the electron-electron collisions to be non-energy-conserving. This is a standard practice in Fokker Planck simulations and does not affect the conclusions regarding predicted ECCD efficiency. The line averaged density and peak electron temperature used in these analyses were chosen to match the typical experimental values of $\approx 1.2 \times 10^{19} m^{-3}$ and 2keV. The explanation for the case of counter ECCD generating net co current drive is that synergistic effects arise between the suprathermal tail produced by the ECRH and the residual toroidal electric field, which readily accelerates these relatively collisionless particles in the co direction, independent of the RF direction. Similar effects have long been recognised in lower hybrid current drive experiments with residual electric field [2] and have also been calculated for ECRH [3]. A sequence of BANDIT-3D analyses reveals the anticipated essentially linear variation with loop voltage of net ECRH-induced current (ie. true RF-driven current plus synergistic current driven by the DC electric field), consistent with ref [3] and shown in figure 7. It should be noted that in the experiment, the toroidal electric field is unlikely to have become independent of minor radius in the plasma, as assumed in these theoretical calculations, due to the duration of the ECRH pulse being a small fraction of the plasma current penetration time. In addition the synergistic effect is sensitive to a number of plasma parameters not well determined in the experiment, so that the modelling results should be taken as illustrative rather than accurate. The bootstrap current is calculated [4] to be approximately 7kA for all the discharges considered here and therefore does not affect the co-counter comparisons.

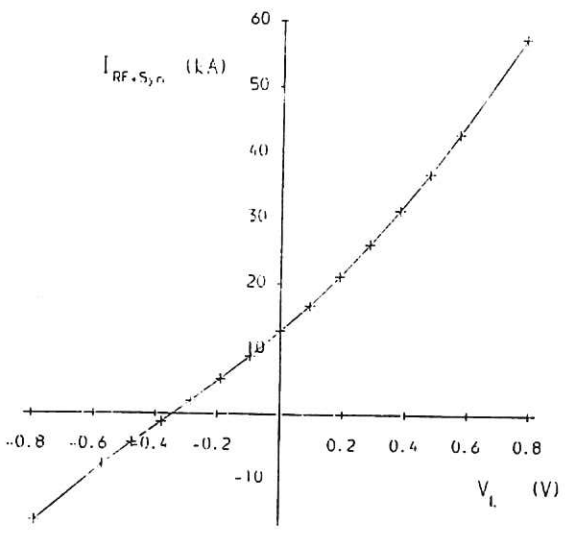

Figure 7. Theoretical variation of RF-induced current with residual loop voltage, showing dominance of the synergistic DC electric field effect at large loop voltages. Sign conventions are as for figure 5.

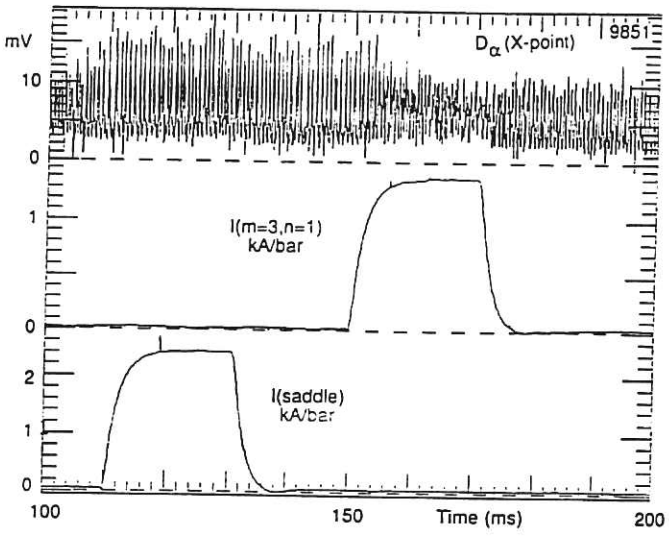

Figure 8. Change in ELM frequency induced by a relatively narrow spectrum "m=3, n=1" RMP field. In this shot the broader spectrum "saddle coil" RMP has no discernible effect. See Figure 9 for the two spectra.

3. ELM Behaviour with Resonant Magnetic Perturbations

H-mode shots in Compass-D exhibit the usual range of characteristics, including ELM's which are manifested in MHD activity, D_α light, outer soft x-ray emission, toroidal rotation of the impurity ions etc. The MHD activity displays a low-m character (m~3) during each main ELM event, although rapidly rotating m~10 bursts are often seen between the ELM's [5]. ELM's represent small but significant plasma current profile relaxations and accordingly create vertical position excursions when present in strongly up-down asymmetric configurations such as the single-null divertor shapes currently used or proposed for JET, ASDEX-U, ITER etc. In addition, ELM frequency is critical to the control of plasma density and impurity retention in present and Next Step devices. It is found on Compass-D that some RMP configurations cause the ELM frequency to increase markedly, eg. precipitating "grassy ELM's" when distinctly separated ELM's prevailed otherwise, see figure 8. At present this effect has been investigated only with two different broad-spectrum RMP configurations, as indicated in figure 9.

Figure 9. Radial profiles of the RMP spectra used in the ELM control experiments

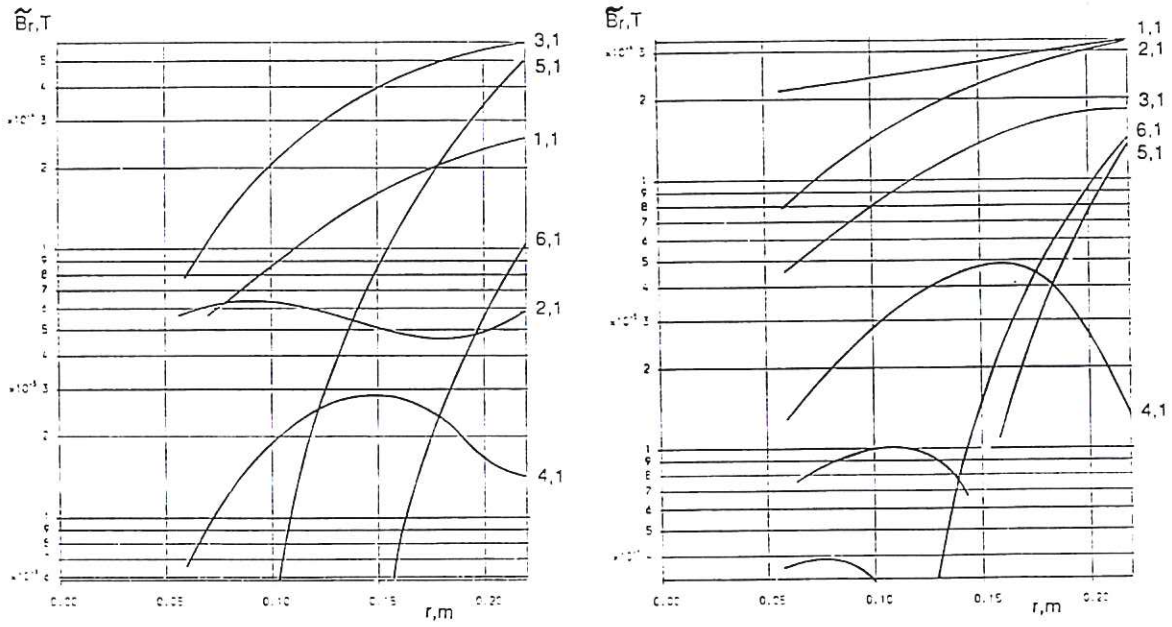

a) "m=3, n=1" configuration

b) "saddle coil" configuration

Although there is some shot to shot variability in the observed effect, no such experiment has so far demonstrated any reduction in ELM frequency. It is as yet unclear whether or not this ELM frequency increase is a direct MHD stabilising effect due to RMP-induced field line tearing and island creation at relevant rational surfaces. An alternative explanation is that the RMP fields cause a change in the plasma edge conditions (such as recycling at the main plasma-surface interaction zones at the divertor target), perhaps independent of any induced tearing close to the plasma periphery.

4. n = 0 Control

The strongly asymmetric SNX configuration currently employed in Compass-D causes small vertical displacements to occur during ELMs, as described above. Occasionally such displacements exceed the recovery capability of the feedback control system, resulting in the rapid development of a Vertical Displacement Event (VDE), as shown in figure 10.

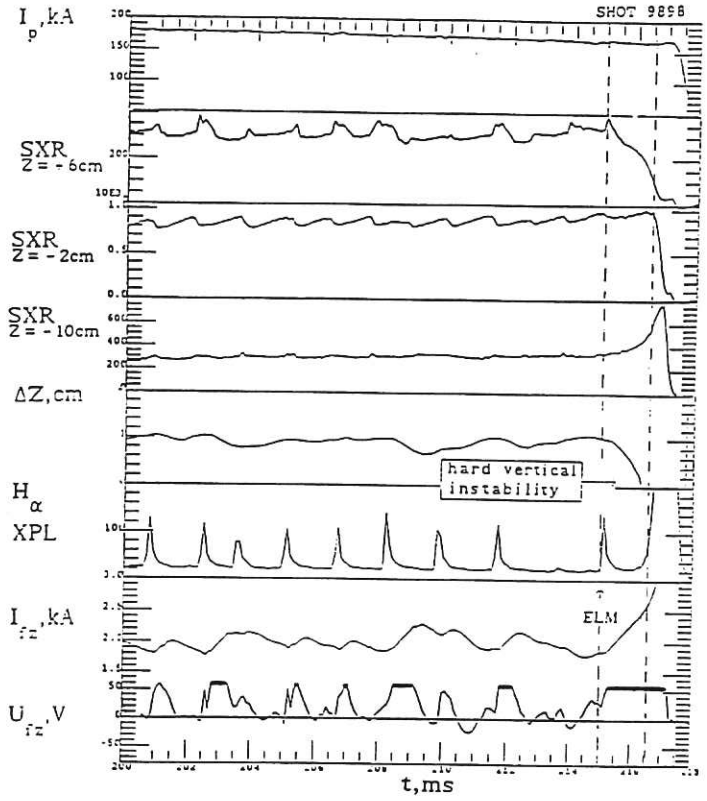

Figure 10. Example of loss of vertical position control caused by the large internal relaxation associated with an ELM (at 215ms). The lowest trace shows the feedback amplifier voltage, with saturations highlighted.

It should be noted that in Compass-D at present, the vertical position control makes use of external flux loops while the vertical velocity control employs only internal poloidal field pick-up coils (to achieve the highest possible speed of response). Both branches of the vertical control feedback are summed into the same power amplifier. Saturation of this feedback amplifier voltage is clearly apparent following most of the ELM's in this data record, although in all but the last such event a stable recovery was achieved (figure 10). Evidently, increasing the feedback amplifier voltage sufficiently would have cured the problem in this case. Nevertheless the issue is pertinent to the control requirements of any significantly asymmetric machine (such as the present EDA version of ITER), unless the ELM's (and other internal relaxations) can be reliably suppressed in amplitude. This might perhaps be achieved by increasing the ELM frequency using appropriate RMP fields as discussed above.

An important issue regarding n=0 control is the accurate determination of the equilibrium parameters of the plasma, especially for strongly shaped configurations. Conventionally a variety of linear analogue signal processing techniques is employed, often equivalent to flux surface extrapolation from magnetic measurement points to the plasma surface. The problem is, however, non-linear, partly due to gradients in the poloidal flux density and partly to the bifurcation of solutions depending on which side of the torus the plasma is limited. One solution is to employ a real-time neural network to process non-linearly an optimised selection of magnetic signals into desired analogue control signals [6]. A prototype scheme of this type has been implemented on Compass-D and is now in routine use for the control of the plasma elongation. A block diagram of the system is shown in figure 11 and comprises a "15-4-3 multilayer perceptron" with the input signals digitally normalised to the plasma current (to allow the network processing capability to concentrate on the non-linear aspects of the problem).

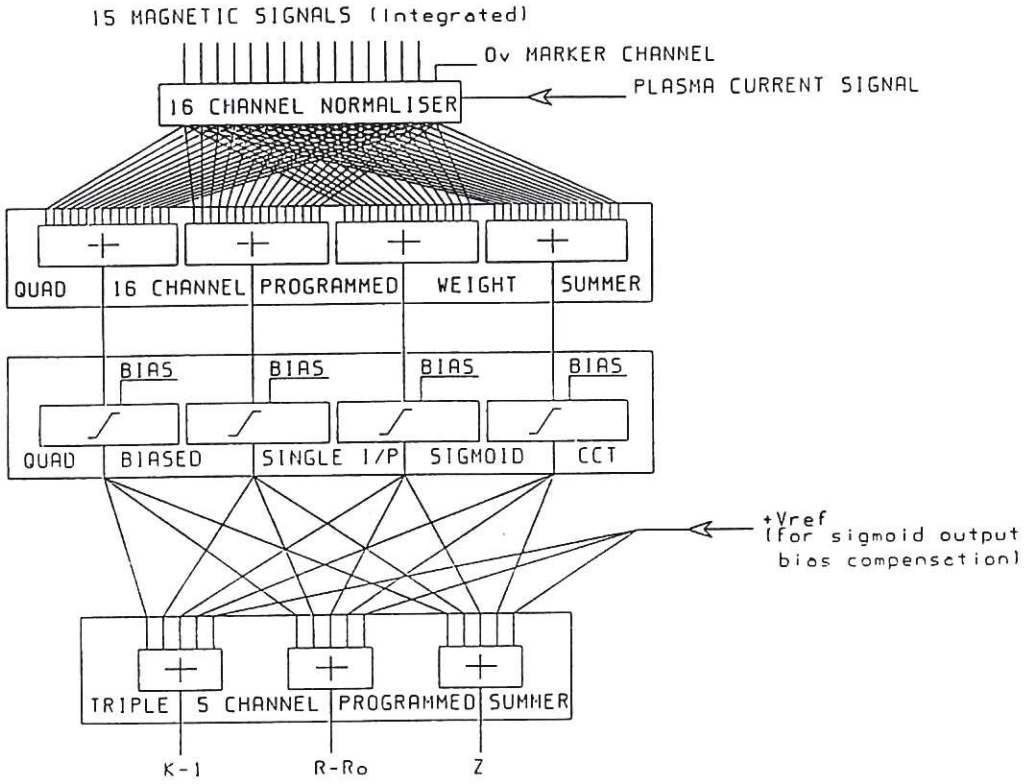

Figure 11. The architecture of the prototype Neural Network used for plasma elongation control in Compass-D.

This device has been trained by software modelling the overall behaviour, using a database of numerically computed equilibria covering the full range of possibilities in Compass-D. The database is divided randomly into two halves, one of which is used to train the network and the other to test it (thus revealing any "overfitting" effects in the training). The database included eight extremes of shaping coil configuration and a large number of ratios of shaping current to plasma current. The network accordingly tracks the plasma behaviour from initiation to extinction, with results presently invalid only when large toroidal currents are flowing in the vacuum vessel. The predicted accuracy is shown in figure 12 and waveforms of a particular test shot are given in figure 13, including comparative results from filament and Grad-Shafranov equilibrium codes. The accuracy of the prototype scheme is limited by the information "bottleneck" of the middle (or "hidden") layer of non-linear elements, in this case only four in number. Even so, the network performs well with the present simple architecture. An analogue bandwidth ≈150kHz is achieved, which is believed to be more than adequate for any n=0 control applications in Compass-D (where the open loop growth rate of the vertical instability is typically ≤10/ms). The prototype scheme will soon be extended to "32-16-16" architecture, allowing much greater accuracy and a wider range of output parameters to be achieved. Further refinements in the choice of input signals will also be made to optimise speed (limited by vessel penetration effects for the external flux loops), as well as accuracy. Recently local magnetic diagnostics have been incorporated into some of the divertor armour tiles, allowing more accurate feedback control of the strike zones and/or the position of the X-point using the neural network, once it has been trained to recognise the new signals.

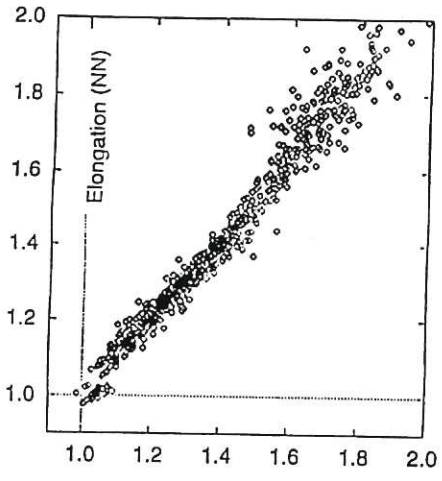

Figure 12. Scatter diagram comprising database values of elongation compared to the predictions of software modelling of the prototype neural network

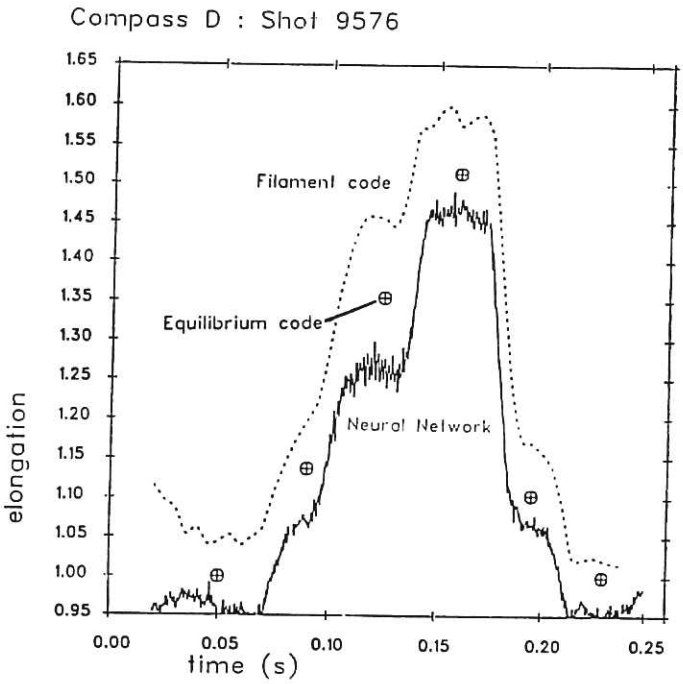

Figure 13. Waveforms of shot 9576, in which the reference waveform for elongation (not shown) was given several steps and the neural network output signal drove the plasma shaping feedback loop. The neural network output is compared with that from a simple filament code and a full equilibrium code.

5. Conclusions

X-mode fundamental resonance ECR current drive experiments in Compass-D clearly reveal a significant RF-induced current, of approximately .03A/W and in contrast to some recent "null result" ECCD experiments elsewhere [7]. This is broadly consistent with 3D Fokker Planck modelling of the RF absorption and velocity-space diffusion processes, but only when synergistic effects between the residual toroidal electric field and the fast perpendicular tail of the electron distribution function are accounted for. These effects are readily seen to produce net "co" current production, even in some cases of "counter" current drive experiments.

Preliminary experiments in ELM control using resonant magnetic perturbation fields reveal a clearly measurable effect but interpretation of the results (and hence refinement of the technique) has only just begun. If reliable, a scheme should then become available for suppressing ELM relaxation amplitude, which would ease n=0 control problems generic to non-symmetric tokamaks and already seen in, for example,Compass-D and ASDEX-U [8].

An electronic neural network has been demonstrated for the first time in the feedback control loop of a tokamak, in this case controlling elongation throughout the discharge while simultaneously monitoring horizontal and vertical plasma position.

The future plans of Compass-D include the implementation of 2MW of 60GHz ECRH, evenly divided between high and low field side launch, and a 300kW 1.3GHz lower hybrid current drive system. These will permit higher power ECR current drive experiments in both fundamental and second harmonic configurations, as well as extending the synergy studies to include lower hybrid wave effects. These RF systems and the four quadrant RMP windings will be used to investigate a variety of techniques for MHD control. Particular attention will be focused on the control or softening of ELM's and major disruptions, the suppression of RMP-induced locked modes by localised ECCD and the spreading of divertor heat flux by creating a swept ergodic magnetic field structure at the plasma boundary.

This work was partially supported by the UK Department of Trade and Industry.

6. References

[1] O'Brien, M et al 1992 *Proc. of IAEA TCM on Advances in Simulation and Modelling of Thermonuclear Plasma* (Montreal) p 527.

[2] Karney, CFF et al 1985 *Phy Rev.A, General Physics*, **32** p 2554.

[3] Start, DFH 1983 *Plasma Physics* **25** p 793

[4] Wilson, HR 1992 *Nuclear Fusion* **32** p 257

[5] Hugill, J et al 1993 *Ohmic H-modes in Compass-D*, 20th EPS Conference Post-deadline paper, to be published.

[6] Bishop, CM et al 1992 *Hardware Implementation of a Neural Network for Plasma Position Control in Compass-D*, 17th SOFT Conference

[7] Alikaev,VV and Parail 1991 VV *Plasma Physics and Controlled Fusion* **33** p 1639

[8] Gruber O et al 1993 *Vertical Displacement Event and Halo Current* 20th EPS Conference